Available online at www.sciencedirect.com
SCIENCE DIRECT
Biomaterials 27 (2006) 3863–3874
Biomaterials
www.elsevier.com/locate/biomaterials

Effect of RGD secondary structure and the synergy site PHSRN on cell adhesion, spreading and specific integrin engagement

Sarah E. Ochsenhirt[a], Efrosini Kokkoli[a], James B. McCarthy[b], Matthew Tirrell[c,*]

[a]Department of Chemical Engineering and Materials Science, University of Minnesota, Minneapolis, MN 55455, USA
[b]Department of Laboratory Medicine and Pathology, University of Minnesota, Minneapolis, MN 55455, USA
[c]Department of Chemical Engineering, University of California, Santa Barbara, CA 93106, USA

Received 7 July 2005; accepted 14 December 2005
Available online 24 March 2006

Abstract

The relationship between the form of cell adhesion, ligand presentation, and cell receptor function was characterized using model Langmuir–Blodgett supported films, containing lipid-conjugated peptide ligands, in which isolated variables of the ligand presentation were systematically altered. First, the conformation of an adhesive Arginine–Glycine–Aspartic acid (RGD) peptide was varied by synthesizing linear and looped RGD peptide-containing amphiphiles and subsequently measuring the impact on the function of human umbilical vein endothelial cells. Secondly, the contribution of non-contiguous ligands to cellular engagement was assessed using multi-component biomimetic films. The peptide amphiphiles were composed of fibronectin-derived headgroups—GRGDSP, and its synergy site Pro–His–Ser–Arg–Asn (PHSRN)—attached to hydrocarbon tails. The peptide amphiphiles were diluted using polyethylene glycol (PEG) amphiphiles, where PEG inhibited non-specific cell adhesion. Cells adhered and spread on GRGDSP/PEG systems in a dose-dependent manner. The presentation of GRGDSP influenced integrin cell surface receptor specificity. Results demonstrated that β_1-containing integrins mediated adhesion to the linear GRGDSP presentation to a greater extent than did the $\alpha_v\beta_3$ integrin, and looped GRGDSP preferentially engaged $\alpha_v\beta_3$. GRGDSP/PHSRN/PEG mixtures that closely mimicked the RGD–PHSRN distance in fibronectin, enhanced cell spreading over their two-component analogues. This study demonstrated that controlling the microenvironment of the cell was essential for biomimetics to modulate specific binding and subsequent signaling events.

Keywords: Looped RGD; Cyclic RGD; PHSRN; HUVEC; $\alpha5\beta1$ integrin; $\alpha_v\beta_3$ integrin

1. Introduction

Control of the microenvironment of the cell provides the biomaterials engineer with the opportunity to modulate cellular events such as growth, differentiation, and angiogenesis, influence supramolecular structures in tissue development; it provides the molecular biologist a means to connect extracellular interactions with biochemical events within the cytoplasm and nucleus of the cell [1]. Consequently, a maturing theme in the biomaterials field is the design, synthesis, and modification of materials that selectively interact with cells through specific biomolecular recognition events [2]. A wide range of techniques in which the microenvironment of the cell is controlled and the biomaterial interface is rendered bioactive, are being employed to create functionalized substrates [3]. A promising approach is the biomimetic modification of the material in which peptides containing the adhesion domains of extracellular matrix proteins are attached to the interface [3,4].

One of the most commonly used ligand in biomaterials and the most physiologically ubiquitous binding motif is the short peptide sequence arginine–glycine–aspartic acid (RGD) [5]. RGD was identified through competitive binding assays involving the integrin family of cell surface receptors. Studies have shown that RGD-modified interfaces can promote integrin-mediated adhesion and migration [3,6]. Additional peptides, such as REDV [7], PHSRN [8] and KNEED [9,10] from fibronectin, YIGSR from

*Corresponding author. Tel.: +1 8058933141; fax: +1 8058938124.
E-mail address: tirrell@engineering.ucsb.edu (M. Tirrell).

0142-9612/$ - see front matter © 2006 Elsevier Ltd. All rights reserved.
doi:10.1016/j.biomaterials.2005.12.012

laminin [11], and FHRRIKA from heparin [12], have been explored when the peptide confers a specific advantage to the substrate or serves as a new design paradigm.

Immobilization strategies have exploited RGD peptide presentation as a means to alter the bioactivity of a substrate. Crystallization of the III_7–III_{10} repeats of fibronectin showed that the RGD in the 10th III repeat is presented in a looped structure that extends 10 Å away from the face of the protein [13]; thus, additional specificity and activity may be imbedded in the peptide structure and presentation. Studies have shown that a more constrained, cyclic or looped, peptide versus a linear one exhibits a higher affinity for the $\alpha_v\beta_3$ and $\alpha_3\beta_1$ integrins [14–17]. This hypothesis was originally suggested by Pierschbacher and Ruoslahti [18]. Additionally, at neutral pH cyclic RGD is more stable than linear RGD in solution [19], and cyclization of linear peptides improves stability against enzymatic degradation [20].

Recently, multi-component peptide systems containing both RGD (the primary recognition site for $\alpha_5\beta_1$ integrins, in fibronectin III_{10} repeat) and PHSRN (the synergy site for $\alpha_5\beta_1$, in fibronectin III_9 repeat), demonstrated that a more complex biomaterial interface is capable of providing increased $\alpha_5\beta_1$-mediated adhesion and instructing the cells to adhere, spread, differentiate, migrate, and mineralize more effectively than RGD alone [21–31].

The Langmuir–Blodgett (LB) technique was used in this study to create highly structured supported membranes with multiple adhesive peptide amphiphiles. The peptide amphiphile structure includes dialkyl ester tails that allow control over their length (C_{16} or C_{18}), a glutamic acid (Glu) linker, a $-(CH_2)_2-$ spacer and a headgroup that contains the bioactive sequence. The tails serve to align the peptide strands and provide a hydrophobic surface for self-association and interaction with other hydrophobic surfaces [32]. LB films incorporating peptide amphiphiles represent a model experimental system to study ligand–receptor interactions with several advantages over other surface immobilization methods. For example, the LB technique allows for precise control of peptide surface density and orientation, mixing of multi-component systems, and the possibility of potential peptide denaturation is minimal because the functionalized surface is created by physical deposition rather than chemical reaction.

Using the LB technique, membranes supported on mica were created here, where the peptide headgroups were presented on the exterior face of the bilayer. Peptide amphiphiles that mimic the adhesion domain of the extracellular protein fibronectin, were constructed from mixtures of peptide amphiphiles and polyethylene glycol (PEG) amphiphilic molecules. PEG has been used extensively as material that is non-adhesive to biological molecules [33,34], and is utilized here to dilute the surface concentration of the peptide amphiphile. LB isotherms were used to verify that the synthesized peptide amphiphiles formed stable supported bilayers. The resulting biofunctional surfaces facilitated the study of cell adhesion phenomena. Cell adhesion, spreading, and receptor specificity experiments independently explored how human umbilical vein endothelial cells (HUVEC) responded to different presentations of multi-component systems of linear and looped GRGDSP, PHSRN, and PEG amphiphiles. Adhesion and spreading of HUVEC on supported bilayers utilized macroscopic measurements of cell number and cell area, respectively. The identity of the integrins engaged by the peptide-functionalized LB film was also examined. Many of the integrins, heterodimeric cell surface receptors ($\alpha_x\beta_y$), recognize the RGD motif; accordingly, the relationship between GRGDSP presentation and the identity of α- and β-subunits were explored using antibody-based inhibition assays.

2. Materials and methods

2.1. Fabrication of supported Langmuir–Blodgett films

The following sequences were synthesized as described elsewhere [32]:

$(C_{16})_2$–Glu–C_2–KAbuGRGDSPAbuK referred to as $(C_{16})_2$GRGDSP;
$(C_{18})_2$–Glu–C_2–KAbuGRGDSPAbuK referred to as $(C_{18})_2$GRGDSP;
$(C_{18})_2$–Glu–C_2–DPKAbuKGGRAbuS referred to as $(C_{18})_2$scr (GRGDSP);
$(C_{18})_2$–Glu–C_2–PHSRN referred to as $(C_{18})_2$PHSRN;
$(C_{16})_2$–Glu–C_2–KAbuGRGDSPAbuK–C_2–Glu–$(C_{16})_2$ referred to as $(C_{16})_2$GRGDSP$(C_{16})_2$;
$(C_{18})_2$−Glu–C_2–KAbuGRGDSPAbuK–C_2–Glu(C_{18}) referred to as $(C_{18})_2$GRGDSP$(C_{18})_2$;
$(C_{18})_2$–Glu–C_2–KDAbuSGAbuGRPK–C_2–Glu$(C_{18})_2$ referred to as $(C_{18})_2$scr(GRGDSP)$(C_{18})_2$, signifying a scrambled sequence.

Before assays were performed, mica disks, 15 mm in diameter, were cut, cleaved, and washed with chloroform, methanol, and MQ water. LB film depositions were done on a KSV 5000 LB system (KSV Instruments, Helsinki, Finland). Predetermined volumes (80–100 μl) of prepared solutions of amphiphilic molecules (~1.0 mg/ml) were spread on the air–water interface and allowed to evaporate for 15 min. All the depositions were done at 40 mN/m. Deposition speed for both the up and down strokes was 1 mm/min. 1,2-Distearoyl-sn-glycero-3-phosphatidylethanolamine (DSPE) (Avanti Polar Lipids, Inc., Alabaster, AL) layer was deposited first on the upstroke to make mica surfaces hydrophobic. The second layer with peptide amphiphiles and their mixtures with PEG (polyethylene glycol with molecular weight 120 covalently linked to DSPE) (Avanti Polar Lipids, Inc., Alabaster, AL), was deposited on the down stroke. Transfer ratios for both layers were calculated to be in the range 0.8–1, indicating that monolayers were deposited on mica surfaces with minimal disruption. The resulting supported membranes were transferred into glass holders under water. Care was taken to avoid exposing the surface to air, as they rearrange to form multilayers [35]. Before cell assays were performed, the MQ water in which the LB surfaces had been deposited was exchanged for a medium that would support cell adhesion (i.e., osmotically acceptable). All assays were performed in endothelial cell basal medium-2 (EBM-2), purchased from Clonetics, Inc., supplemented with 0.1% bovine serum albumin (BSA) (EBM-2 + 0.1% BSA). The glass holders with the LB films were placed in a CoStar® (VWR, Inc.) 12-well plates and incubated at 37 °C and 5% CO_2 for 2 h, prior to starting the assay.

2.2. Preparation of protein substrates

A 1% concentrated solution of BSA (Sigma) in PBS was prepared and stored at 4 °C. The day before an assay, a sample of the 1% BSA in PBS solution was diluted using sterile PBS to a concentration of 0.1% BSA. The solution was added to appropriate wells of a 12-well plate. Fibronectin, and vitronectin (Chemicon International, Inc.) were received as concentrated aliquots. One day prior to the cell assay, a sample of the protein solution was diluted using sterile PBS. A spectrophotometer determined the protein concentration. After a 10 μg/ml solution of protein in PBS was prepared, a known volume was placed in select wells of a 12-well plate. The plates with the BSA, fibronectin and vitronectin proteins were covered with parafilm and placed in the 5% CO_2 incubator overnight at 37 °C. The following morning, the plates were washed using PBS to remove non-adsorbed protein. After removal of excess PBS, 1.5 ml of EBM-2 + 0.1% BSA was added. The volume added approximated the volume of EBM-2 + 0.1% BSA contained in the glass holder containing each LB film. At this point, the assay protocols were identical for both the protein controls and the LB films.

2.3. Cell culture and release

Cryopreserved passage 1 HUVEC and all media, growth supplements, and passaging solutions were purchased from Clonetics, Inc. (San Diego, CA.). HUVEC were cultured as per instructions of Clonetics, Inc. at 37 °C in a 5% CO_2 atmosphere. In brief, HUVEC were maintained in endothelial growth medium-2 (EGM-2), containing proprietary concentrations of fetal bovine serum, hydrocortisone, human fibroblast growth hormone, vascular endothelial cell growth factor, R3-immunoglobulin factor, ascorbic acid, human epithelial growth factor, GA-1000, and heparin. Cells were passaged using HEPES buffered saline solution (HBSS), trypsin/EDTA, and trypsin neutralizing solution (TNS). Cells used for adhesion studies were in passages 3–4. After passage 5, cells often entered a quiescent phase and failed to proliferate. In a laminar flowhood 80% confluent monolayers of HUVEC cells were rinsed with HBSS (Clonetics, Inc.) and then incubated with trypsin/EDTA (Clonetics, Inc.) at 37 °C until HUVEC had rounded up. TNS was added to each flask to inhibit the proteolytic activity of trypsin. After releasing the cells were pelleted and washed with endothelial cell basal medium-2 (EBM-2) supplemented with 0.1% BSA (EBM-2 + 0.1% BSA) to remove remaining serum proteins. The cell pellet was then resuspended in 1 ml of EBM-2 + 0.1%BSA. A small volume was removed from the well-mixed cell suspension and cells were counted.

2.4. Adhesion assay

After calculating the total number of cells in the cell suspension, the fluorescent probe Calcein AM® (Molecular Probes) was added to the cell suspension. The solution was incubated at 37 °C for 20 min, with frequent agitation. Cells were pelleted and washed using EBM-2 + 0.1% BSA. After the final wash, the pellet was resuspended using EBM-2 + 0.1% BSA to yield a final concentration of 1.0×10^6 cells/ml. After mixing the suspension well, a calibration standard was created. Using a calibrated pipetman, 10^5 cells were plated onto each LB film or protein-coated surface. After adding cells, the 12-well plate was gently shaken to distribute the cells evenly across the substrate and placed in the 5% CO_2 incubator at 37 °C for the duration of the adhesion assay—30 or 60 min, as noted in the caption for each data set.

At the conclusion of the experiment, cells on adsorbed protein substrates were gently washed and aspirated using EBM-2 + 0.1%BSA. Cells on LB films were washed carefully making sure that films were not exposed to air, by using tweezers to transfer the disk from the glass holder and gently lower and raise the disk through a small volume of EBM-2 + 0.1%BSA. All cells were lysed and the fluorescence was measured using a standard plate reader. The calibration standard converted fluorescence intensity to the percentage of cells originally plated on the surfaces that had adhered to that surface. Within each experiment, each condition was performed in triplicate. Each experiment was performed in duplicate.

2.5. Spreading assay

After calculating the total number of cells in the cell suspension, the suspension was diluted using EBM-2 + 0.1%BSA to a final concentration of 1.0×10^6 cells/ml. After mixing the suspension well, a calibrated pipetman was used to pipet 10^5 cells onto each LB film. The 12-well plate was gently shaken to distribute the cells evenly across the substrate and then placed in the 5% CO_2 incubator at 37 °C for the duration of the spreading assay—30 or 60 min, as noted in the caption for each data set. At the end of the experiment, the surfaces were washed as previously described. The cells were fixed and stained using either Diff-Quik staining solutions (Baxter Scientific Products) or 3.7% formaldehyde in PBS, 0.1% Triton X-100 in PBS, and rhodamine–phalloidin solutions (Molecular Probes). Surfaces stained using Diff-Quik solutions were imaged using a Nikon microscope and NIH Image software, while surfaces stained with the rhodamine–phalloidin series were imaged using a Nikon microscope equipped with a laser and Metamorph software. Phalloidin stains the cytoskeletal component f-actin. A minimum of 200 cells per surface were imaged, where each condition was performed in triplicate and each experiment in duplicate.

2.6. Inhibition assay

Integrin blocking monoclonal antibodies were used to identify which integrin(s) or subunit(s) mediated adhesion. To block adhesion, anti-β_1 (P5D2), and anti-$\alpha_v\beta_3$ (LM609) monoclonal antibodies (Chemicon International, Inc.) were used. As a control antibody, IgG1 K was used because it is an isotype match to both P5D2 and LM609. After calculating the total number of cells in the cell suspension, the fluorescent probe Calcein AM® (Molecular Probes) was added to the cell suspension. The solution was incubated at 37 °C for 20 min, with frequent agitation. Cells were pelleted and washed using EBM-2 + 0.1% BSA. After the final wash, the pellet was resuspended using EBM-2 + 0.1% BSA. A volume of the adjusted cell suspension, selected antibody, and EBM-2 + 0.1% BSA were placed in a polystyrene conical and incubated for 20 min at 37 °C with frequent agitation. After mixing the suspension well, a calibrated volume was pipeted onto each LB film or protein-coated surface. The volumes and concentrations of all reagents were predetermined to yield a final antibody concentration of either 10 or 20 μg/ml, as needed. After creating a calibration standard and pipeting the cells onto the experimental substrates, each 12-well plate was gently shaken to distribute the cells evenly across the substrate. The plates were then placed in the 5% CO_2 incubator at 37 °C for the duration of the inhibition assay. At the conclusion of the experiment, cells on LB films were washed as previously described. All cells were lysed and the fluorescence was measured using a standard plate reader. The calibration standard converted fluorescence intensity to the percentage of cells originally placed on the surfaces that adhered to the surface. Within each experiment, each condition was performed in triplicate. Each experiment was performed in duplicate.

3. Results and discussion

3.1. LB isotherms

The surface pressure-area isotherms for mixtures of linear $(C_{18})_2$GRGDSP and PEG amphiphiles recorded at room temperature are shown in Fig. 1. The $(C_{18})_2$GRGDSP isotherm exhibited an extended liquid phase, because of molecular interactions between neighboring amphiphiles, and a secondary transition that occurred at about 0.75 nm^2/mol and $\pi = 20$ mN/m.

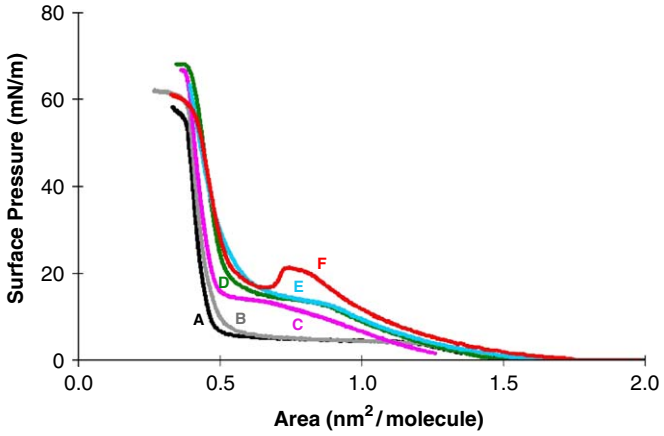

Fig. 1. Surface pressure–area isotherms of mixtures of $(C_{18})_2$GRGDSP/PEG on MQ water subphase at room temperature. (A) PEG. (B) 10 mol% $(C_{18})_2$GRGDSP—90 mol% PEG. (C) 25 mol% $(C_{18})_2$GRGDSP—75 mol% PEG. (D) 50 mol% $(C_{18})_2$GRGDSP—50 mol% PEG. (E) 75 mol% $(C_{18})_2$GRGDSP—25 mol% PEG. (F) $(C_{18})_2$GRGDSP.

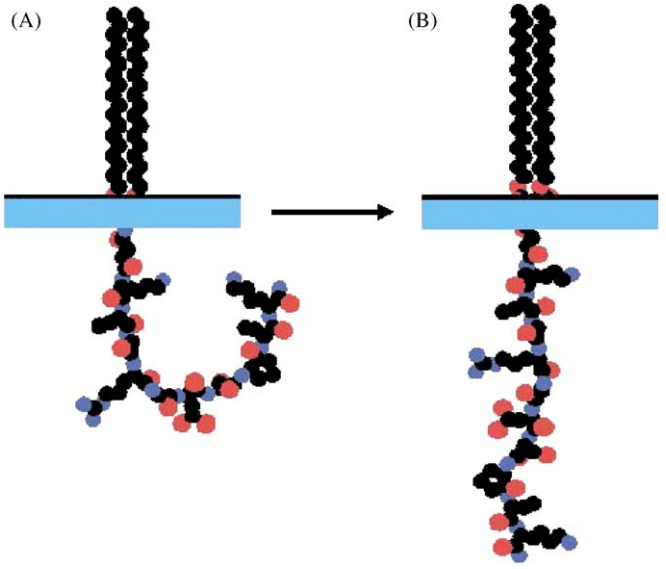

Fig. 2. Hypothetical secondary transition of peptide amphiphiles. Visualization of structural changes in the peptide headgroup that would potentially explain the observed secondary transition for $(C_{18})_2$GRGDSP in Fig. 1F. (A) The peptide headgroup has a folded/bent conformation. (B) The peptide headgroup is in an extended conformation.

This "hump" may be due to a secondary transition of the peptide headgroup. At large areas per molecule and in an ideal monolayer, the hydrocarbon tails would have been able to sample large areas before interactions between neighboring tails occurred. At these long ranges, the peptide headgroup would have had plenty of space to occupy a folded or bent conformation (Fig. 2A). As the area per molecule was reduced and the tails aligned, less space would have been available for the folded/bent peptide headgroup. Depending on the position of the residues in the bent conformation, the headgroups could sterically and/or electrostatically repel one another and thus the peptide may unfold to occupy a more extended state (Fig. 2B) as a means to relax the repulsions between headgroups. After the peptide headgroup had extended the tails would have been free to align and form a solid-like monolayer of closely packed tails. In summary, at areas per molecule larger than 0.75 nm^2/dialkyl tail, the $(C_{18})_2$GRGDSP headgroup may occupy a bent or folded conformation (Fig. 2A), while at areas smaller than 0.75 nm^2/dialkyl tail, the peptide may occupy an extended conformation (Fig. 2B).

Molar mixtures of the pure PEG molecule and $(C_{18})_2$GRGDSP amphiphiles (Fig. 1) revealed that as the molar percentage of $(C_{18})_2$GRGDSP increased, the isotherm transitioned from one resembling PEG (Fig. 1A) to one resembling $(C_{18})_2$GRGDSP (Fig. 1F). A mixture of 10 mol% $(C_{18})_2$GRGDSP/90 mol% PEG (Fig. 1B) almost duplicated the isotherm of pure PEG, whereas 50/50 (Fig. 1D) and 75/25 mol% (Fig. 1E) mixtures of the two amphiphiles yielded isotherms that more closely resembled that of pure $(C_{18})_2$GRGDSP (Fig. 1F). In the mixtures that contained higher molar percentages of $(C_{18})_2$GRGDSP, distinct changes in the slope of the isotherms occurred at the same area per molecule as the secondary transition occurred in the pure monolayer. This might suggest that in the mixed monolayers the peptide headgroups underwent a similar change in state or conformation, but that the presence of the PEG dampened the severity of the transition and yielded a muted slope change.

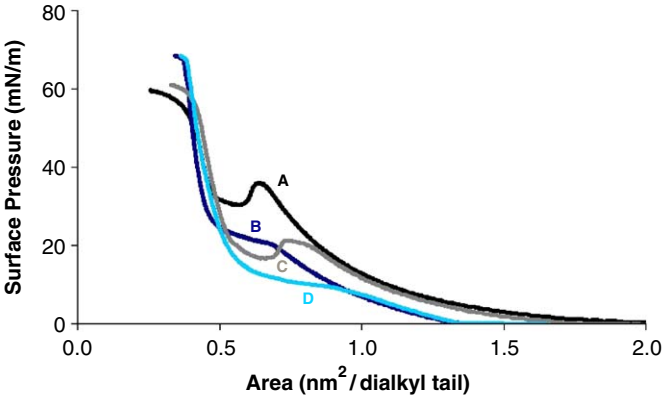

Fig. 3. Surface pressure–area isotherms of linear and looped GRGDSP peptide-amphiphiles on MQ water subphase at room temperature. (A) $(C_{16})_2$GRGDSP. (B) $(C_{16})_2$GRGDSP$(C_{16})_2$. (C) $(C_{18})_2$GRGDSP. (D) $(C_{18})_2$GRGDSP$(C_{18})_2$.

Dialkyl tails were attached to both the *N*-α-amine and the ε-amine of the C-terminal lysine of the KAbuGRGDSPAbuK peptide. When the amphiphiles were deposited, both sets of dialkyl tails were energetically driven to insertion in the hydrophobic bilayer, which yielded a looped presentation of the GRGDSP at the interface. Two looped GRGDSP amphiphiles were synthesized. One had hydrocarbon tails of 16 units, while the other had tails of 18 units. The two molecules, $(C_{16})_2$GRGDSP$(C_{16})_2$ and $(C_{18})_2$GRGDSP$(C_{18})_2$, were designed for direct comparison to their linear analogues. Fig. 3 shows how the pure monolayers of the linear and looped amphiphiles compared

with respect to GRGDSP presentation and tail length. The isotherms of $(C_{16})_2$GRGDSP$(C_{16})_2$ (Fig. 3B) and $(C_{18})_2$GRGDSP$(C_{18})_2$ (Fig. 3D) exhibited a large expanded phase, a solid like regime, and an extremely high collapse pressure. A change in slope occurred within both $(C_{16})_2$GRGDSP$(C_{16})_2$ (Fig. 3B) and $(C_{18})_2$GRGDSP$(C_{18})_2$ (Fig. 3D) isotherms at approximately the same area per dialkyl tail as did the secondary transition in the analogous linear $(C_{16})_2$GRGDSP (Fig. 3A) and $(C_{18})_2$GRGDSP (Fig. 3C) amphiphiles. For the looped amphiphiles, the peptide headgroup may have attempted to modify its conformation to minimize unfavorable electrostatic interactions, but no transition was observed because the second dialkyl tail reduced the number of degrees of freedom available to the peptide headgroup. Additionally, the architecture of the loop itself may have changed to alleviate some of the steric/electrostatic strain inherent in the peptide sequence. This is one explanation for the agreement in slope changes in the isotherms of the looped amphiphiles with the secondary transitions in the isotherms of their linear analogues. The longer $(C_{18})_2$ tail length shifted the secondary transition of the linear GRGDSP isotherm, and the change in slope of the looped GRGDSP, to lower surface pressures than the $(C_{16})_2$ tail isotherms. A possible explanation for this is that the increase in the hydrophobic interaction between the $(C_{18})_2$ tails forced the tails to align, and the peptide headgroups to relax to a modified conformation at lower surface pressures than the $(C_{16})_2$ tails.

Mixtures of each looped GRGDSP amphiphile with PEG were recorded (data not shown). The isotherms demonstrated the same trends that were observed in the respective mixtures of the linear analogues with PEG. Succinctly, at lower concentrations of the looped peptide amphiphile the isotherms resembled PEG, while at higher concentrations the isotherms resembled that of the pure looped amphiphile.

3.2. Effect of RGD secondary structure on cell adhesion

HUVEC adhered to mixed monolayers of GRGDSP peptide amphiphiles and PEG amphiphiles (Fig. 4A). The contribution of GRGDSP presentation was investigated by using $(C_{16})_2$GRGDSP and $(C_{16})_2$GRGDSP$(C_{16})_2$ independently to yield substrates that presented the peptide in an N-tethered linear form and an N- and C-tethered loop. The contribution of ligand density to cell adhesion was studied by depositing the GRGDSP and PEG mixtures at two molar concentrations. The "low" concentration was composed of 10 mol% GRGDSP/90 mol% PEG, while the "high" concentration was composed of 75 mol% GRGDSP/25 mol% PEG. For both the linear and looped GRGDSP architectures the percentage of adhering cells increased with GRGDSP surface concentration. Adhesion of HUVEC to 10 mol% $(C_{16})_2$GRGDSP was approximately equal to 10 mol% $(C_{16})_2$GRGDSP$(C_{16})_2$, while adhesion to 75 mol% $(C_{16})_2$GRGDSP appeared to exceed cell adhesion to 75 mol% $(C_{16})_2$GRGDSP$(C_{16})_2$. While the increased adhesion might be immediately attributed to ligand presentation, additional variables, such as height differences and surface coverage should be considered because they may be essential for the interpretation of data.

The height difference between the linear GRGDSP and PEG is about 3 nm. The linear GRGDSP headgroup is approximately 4.4 nm (10 amino acids × 0.37 nm/amino acid [36], plus 0.7 nm for the length of the (Glu) linker and $(CH_2)_2$ spacer [34]), and the PEG headgroup length is

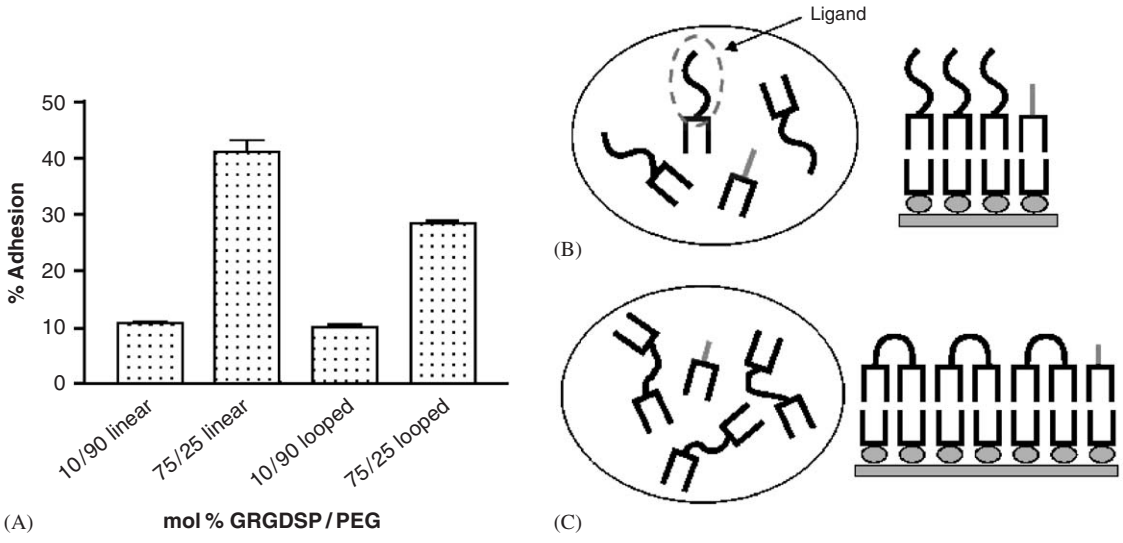

Fig. 4. (A) GRGDSP monolayers support HUVEC adhesion in a concentration-dependant manner. Adhesion of HUVEC to mixed monolayers of $(C_{16})_2$GRGDSP (linear)/PEG and $(C_{16})_2$GRGDSP$(C_{16})_2$ (looped)/PEG after 30 min incubation at 37 °C in basal medium supplemented with 0.1% BSA, where molar concentrations are GRGDSP/PEG ligands at surface (error bars represent S.E.M.). (B–C) Solution and surface concentration versus surface coverage of ligand. Schematics delineating distinctions between solution and surface characteristics of linear (B) and looped (C) peptide amphiphile mixtures where, solution and surface concentrations of linear and looped GRGDSP ligand are 75 mol% GRGDSP/25 mol% PEG, while surface coverage by ligand is 75% linear GRGDSP/25% PEG and 43% looped GRGDSP/14% PEG.

1.6 nm [34]. However, the height of the looped GRGDSP headgroup should be close to the PEG height. Thus, the smaller height difference between looped GRGDSP-PEG compared to linear GRGDSP-PEG could have affected cell adhesion, since it has been shown that height differences between membrane components determine the accessibility of the peptide ligand to the cell surface receptors [34]. When the PEG chains are shorter than the peptide, the peptide is fully exposed at the interface and can be recognized by the receptor, whereas when PEG and the peptide have the same length, the PEG repulsion may mask some of the peptide adhesive properties.

The PEG amphiphile and the linear GRGDSP amphiphile, $(C_{16})_2$GRGDSP, have single dialkyl tails. When this mixture of linear amphiphiles is spread on the air–water interface, the area occupied by each tail contains only one headgroup. The ratio of ligand:tail is 1:1, which results in the ligand density and the surface coverage of ligand being equal. For instance, a solution composition of 75 mol% GRGDSP/25 mol% PEG is created by mixing three molecules of $(C_{16})_2$GRGDSP for every one molecule of PEG (Fig. 4B). When this mixture is compressed on the air–water interface, each linear GRGDSP amphiphile and each PEG amphiphile occupy approximately equal areas. Because the ligand:amphiphile ratio (3:4) remains unchanged from solution to supported monolayer, the surface molar concentration of the GRGDSP/PEG remains 75%/25% for the LB film. Additionally, because each dialkyl tail in the monolayer contains one ligand (either GRGDSP or PEG), GRGDSP covers 75% of the surface (surface coverage is based on a surface of dialkyl tails). However, the surface concentration and surface coverage of $(C_{16})_2$GRGDSP$(C_{16})_2$ and PEG mixtures are not equal. For instance, a solution composition of 75 mol% GRGDSP/25 mol% PEG is created by mixing three molecules of $(C_{16})_2$GRGDSP$(C_{16})_2$ with one molecule of PEG (Fig. 4C). The ratio of GRGDSP ligand:total number of amphiphiles in solution is 3:4. In the LB film, the ratio of GRGDSP ligand:total number of amphiphiles remains 3:4, but the ratio of GRGDSP ligand:dialkyl tail becomes 3:7, where three $(C_{16})_2$GRGDSP$(C_{16})_2$ contribute six dialkyl tails and one PEG contributes one tail. Because the ligand:amphiphile ratio (3:4) remains unchanged from solution to supported monolayer, the surface molar ratio of the GRGDSP/PEG remains 75%/25%. Conversely, because the ratio of GRGDSP ligand:total number of dialkyl tails is 3:7, GRGDSP covers only 43% of the surface, while PEG covers 14% (surface coverage is based on a surface of dialkyl tails). The solution concentration of a $(C_{16})_2$GRGDSP$(C_{16})_2$/PEG mixture is the same as the surface concentration of amphiphiles but not the surface coverage per amphiphile. Thus, the surface coverage of GRGDSP ligands is always greater on a linear GRGDSP film than on a looped GRGDSP film for the same surface/solution concentration. Yet, the data are reported by molar ratios of ligand at the surface rather than as percent surface coverage because the ratio of ligands at the interface is believed to be more important with respect to three-component mixtures. For example, in later experiments with mixtures of GRGDSP/PHSRN/PEG the molar ratio of GRGDSP:PHSRN will be kept 1:1 to accurately mimic fibronectin. Thus, while the ratio of GRGDSP:PHSRN ligand on the surface is always 1:1, the total number of ligands at the interface is dependent on whether $(C_n)_2$GRGDSP or $(C_n)_2$GRGDSP$(C_n)_2$ is used. All data are therefore reported as molar ratios of ligands at the interface.

3.3. Effect of RGD secondary structure on cell spreading

The contribution of peptide presentation to cell spreading was investigated using LB films of $(C_{16})_2$GRGDSP/PEG and $(C_{16})_2$GRGDSP$(C_{16})_2$/PEG mixtures as substrates. The number of cells adhering to supported monolayers of linear and looped GRGDSP/PEG increased with increasing surface concentration of $(C_{16})_2$GRGDSP and $(C_{16})_2$GRGDSP$(C_{16})_2$ (Fig. 4A). Spreading assays were performed to study the morphology/dimensions of the adherent cells. The area of spread HUVEC increased as the surface concentration of $(C_{16})_2$GRGDSP (Fig. 5) and $(C_{16})_2$GRGDSP$(C_{16})_2$ increased (Fig. 6), hence, the dose-dependent increase in cell spreading correlated to the dose-dependent increase in cell adhesion (Fig. 4A). HUVEC did not spread on LB films of $(C_{18})_2$scr(GRGDSP) occupying an area of approximately 160 μm^2. Therefore, the increase in cell area with respect to increased surface concentration of linear and looped GRGDSP was attributed to specific interactions between GRGDSP and integrin receptors. Clearly HUVEC adhered and spread in a concentration-dependent manner on immobilized linear and looped GRGDSP peptides.

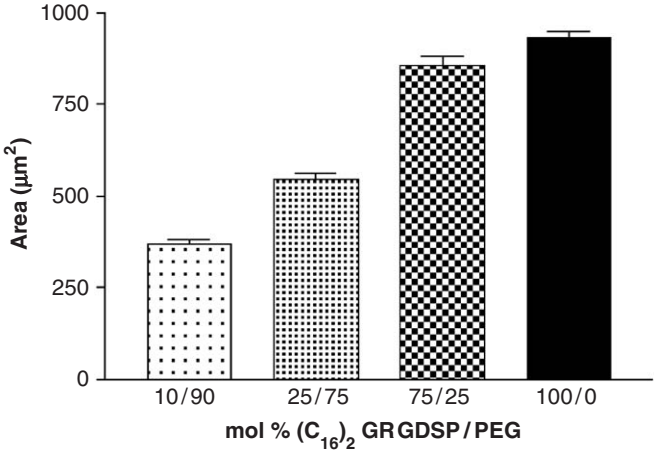

Fig. 5. Dose-dependent spreading on linear GRGDSP amphiphile. Area of spread HUVEC to supported mixed monolayers of $(C_{16})_2$GRGDSP and PEG after 60 min incubation at 37 °C in basal medium supplemented with 0.1% BSA (error bars represent S.E.M.).

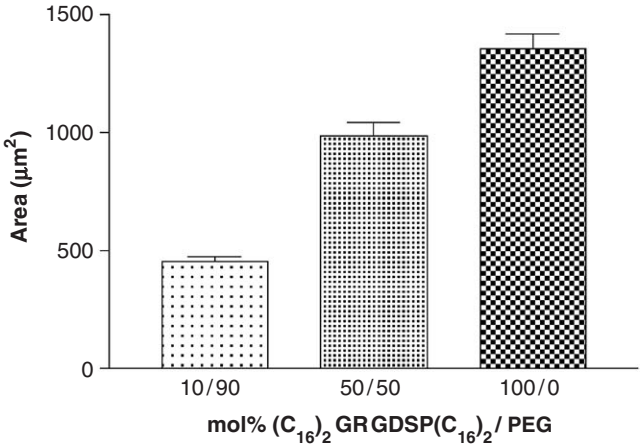

Fig. 6. Dose-dependent spreading on looped GRGDSP amphiphiles. Area of spread HUVEC to supported mixed monolayers of $(C_{16})_2$GRGDSP$(C_{16})_2$ and PEG after 60 min incubation at 37 °C in basal medium supplemented with 0.1% BSA (error bars represent S.E.M.).

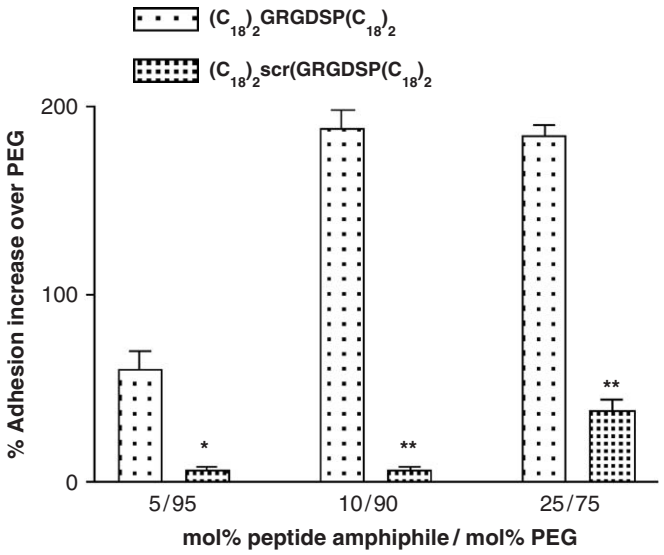

Fig. 7. GRGDSP specificity. Comparison of HUVEC adhesion to supported mixed monolayers of looped peptide amphiphiles and PEG, where the peptide amphiphiles were $(C_{18})_2$GRGDSP$(C_{18})_2$ and the control $(C_{18})_2$scr(GRGDSP)$(C_{18})_2$ after 30 min incubation at 37 °C in basal medium supplemented with 0.1% BSA (error bars represent S.E.M.). Adhesion is presented as percent increase over HUVEC adhesion to a pure monolayer of PEG. $p_{5/95} < 0.002$, $p_{10/90} < 0.001$, $p_{25/75} < 0.001$.

3.4. Effect of RGD secondary structure on integrin specificity

To investigate specificity, the degree of cell adhesion on GRGDSP and scr(GRGDSP) was examined for various mixtures of the two peptide amphiphiles and PEG. At each concentration of peptide amphiphile/PEG, a statistically greater number of cells adhered to mixtures composed of $(C_{18})_2$GRGDSP$(C_{18})_2$ than $(C_{18})_2$scr(GRGDSP)$(C_{18})_2$ (Fig. 7). The data is presented as a percent increase over HUVEC adhesion to a PEG monolayer, which served as a negative control. HUVEC adhesion on various mixtures of linear GRGDSP/PEG and linear scr(GRGDSP)/PEG was also examined. Similar to the looped peptide amphiphiles, at each concentration of linear peptide amphiphile/PEG, a statistically greater number of cells adhered to mixtures composed of $(C_{18})_2$GRGDSP than $(C_{18})_2$scr(GRGDSP) (data not shown). Thus, the data indicated that cellular response was dependent on the amino acid sequence, arguing that the dose-dependent adhesion to $(C_{18})_2$ GRGDSP$(C_{18})_2$ and $(C_{18})_2$GRGDSP was a specific interaction between GRGDSP and cell integrins.

While macroscopic variables such as number of adherent cells and the dimension of spread cells are classical variables to evaluate the bioactivity of a substrate, the overriding question was whether presentation of GRGDSP could modulate the initial binding of HUVEC to GRGDSP-functionalized LB films. Because of this hypothesis, inhibition assays were employed for three reasons: first, to verify that the observed adhesion and spreading data were integrin mediated; second, to identify integrins that recognized the tethered GRGDSP; and third, to determine whether GRGDSP presentation modulated the integrin engagement profile. Prior to the inhibition assays, positive and negative controls verified the activity of the monoclonal antibodies (Fig. 8). BSA and PEG served as negative controls, as did DSPE. Fibronectin and vitronectin were used as positive controls for $\alpha_5\beta_1$ (the fibronectin receptor) and $\alpha_v\beta_3$ (the vitronectin receptor). The anti-integrin monoclonal antibodies were used independently and in combination to evaluate which integrin(s) mediated adhesion to the control substrates and supported GRGDSP/PEG LB films. As a control antibody, IgG1 K,

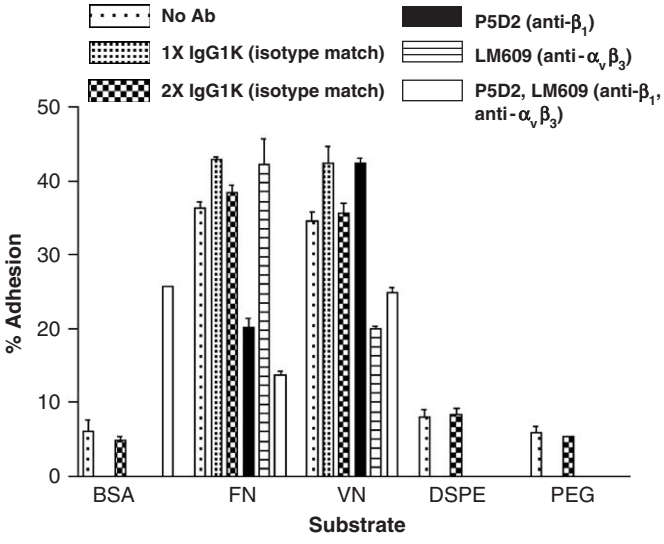

Fig. 8. Protein control inhibition assays. Inhibition assay verifying the specificity and testing the activity of two anti-integrin blocking antibodies, P5D2 anti-β_1 and LM609 anti-$\alpha_v\beta_3$, to inhibit adhesion to substrates of BSA, fibronectin (FN), vitronectin (VN), deposited monolayer of phosphatidylethanolamine (DSPE) and a supported bilayer of PEG after 30 min incubation at 37 °C in basal medium supplemented with 0.1% BSA (error bars represent S.E.M.).

a polyclonal immunoglobulin was used because it is an isotype match to both P5D2 and LM609 and should not affect cell adhesion. Use of an appropriate isotype match verifies that it is the antigen-binding site of the monoclonal antibodies that is specifically interacting with the integrin rather than heavy or light chains. P5D2 and LM609 interacted specifically with the β_1-subunit and $\alpha_v\beta_3$ integrin, respectively (Fig. 8). P5D2 inhibited HUVEC adhesion to fibronectin, but did not affect adhesion to vitronectin, while the converse was true for LM609. The data also showed that even in combination, cell adhesion was reduced to levels similar to those of the appropriate antibody acting independently. The specificity of the inhibition was further verified as cell adhesion was unaffected in the presence of the isotype match control antibody at either concentration. These controls verified the activity and specificity of P5D2 and LM609. When LB films were incorporated into the inhibition assays, the control substrates and antibodies allowed decreases in cell adhesion to be attributed to the β_1 subunit or $\alpha_v\beta_3$ integrin, accordingly.

Two surface concentrations of $(C_{18})_2$GRGDSP/PEG and $(C_{18})_2$GRGDSP$(C_{18})_2$/PEG mixtures were deposited onto the solid support. The "low" concentration was 10 mol% GRGDSP/90 mol% PEG and the "high" concentration was 75 mol% GRGDSP/25 mol% PEG. After incubation in the presence or absence of antibodies, HUVEC were plated onto GRGDSP/PEG LB films to determine which integrins mediated adhesion (Fig. 9). HUVEC adhesion to surfaces of 10 mol% $(C_{18})_2$GRGDSP

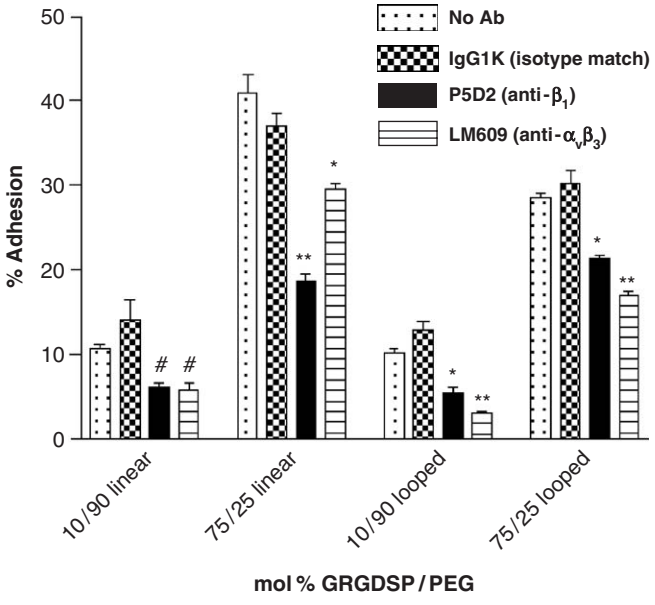

Fig. 9. Inhibition assays using monoclonal anti-integrin antibodies. Inhibition assay using anti-integrin blocking antibodies against β_1 (P5D2) or $\alpha_v\beta_3$ (LM609) to determine integrin engagement profile for HUVEC adhesion to mixed monolayers of $(C_{18})_2$GRGDSP with PEG and $(C_{18})_2$GRGDSP$(C_{18})_2$ with PEG after 30 min incubation at 37 °C in basal medium supplemented with 0.1% BSA (error bars represent S.E.M.). # indicates $p<0.1$, * indicates $p<0.05$, ** indicates $p<0.01$.

$(C_{18})_2$/90 mol% PEG and 75 mol% $(C_{18})_2$GRGDSP$(C_{18})_2$/25 mol% PEG mixtures was inhibited by both P5D2 and LM609, but to a greater extent by LM609 (Fig. 9), suggesting that the looped RGD presentation favored $\alpha_v\beta_3$. Hence, we assert that $\alpha_v\beta_3$ mediated HUVEC adhesion to looped GRGDSP to a significantly greater degree than did the β_1-containing integrins.

HUVEC adhesion to surfaces of 10 mol% $(C_{18})_2$GRGDSP/90 mol% PEG was inhibited equally by P5D2 and LM609, suggesting that the RGD presentation was amenable to both β_1-containing integrins and $\alpha_v\beta_3$. P5D2, however, inhibited HUVEC adhesion to surfaces of 75 mol% $(C_{18})_2$GRGDSP/25 mol% PEG to a significantly greater degree than did LM609, suggesting that at higher GRGDSP surface concentrations, β_1-integrin mediated adhesion was greater than $\alpha_v\beta_3$-integrin mediated adhesion. While the differences in the integrin engagement profiles between the low and high concentrations of the linear GRGDSP could be attributed to the surface concentration, additional variables may have yielded these two integrin profiles. While presentation of tethered GRGDSP depended on the architecture of the peptide amphiphile, once deposited onto a supported monolayer, the presentation of the peptide headgroup was semi-malleable. The tethered headgroup of $(C_{18})_2$GRGDSP was linear, flexible, and capable of sampling numerous conformations to minimize the free energy of the system. The molar ratios of $(C_{18})_2$GRGDSP to PEG could potentially affect mixing. If one concentration yielded a homogenous surface while the other yielded a heterogeneous surface, ligand presentation could differ.

Recent studies have shown that the miscibility profile of linear GRGDSP-containing peptide amphiphiles with PEG, in a two-component film, is concentration dependent [37]. LB films with linear peptide amphiphile concentrations above 40 mol% are mixed whereas smaller contents give rise to phase-separated surfaces with PEG amphiphiles forming the isolated domains and linear peptide amphiphiles the surrounding matrix [37]. This difference in miscibility could have an effect on ligand presentation. In a homogeneous system, such as the high concentration of linear GRGDSP, the peptide ligands would be equidistant from one another. To reduce the free energy of the system, the ligands would adopt the same conformation, resulting in all of the ligands being uniformly presented to the integrins. If the conformational state of the peptide headgroup is selective to one integrin, then a homogeneous surface enhances integrin specificity. However, in a phase-separated LB film, such as the case of the low concentration of linear GRGDSP, where one amphiphile is forming the continuous phase, with the second amphiphile exclusively forming the isolated phase, some GRGDSP ligands would be on the boundary between GRGDSP and PEG phases. The GRGDSP headgroup is approximately 4.4 nm (10 amino acids × 0.37 nm/amino acid [36], plus 0.7 nm for the length of the (Glu) linker and $(CH_2)_2$ spacer [34]), and the PEG headgroup length is 1.6 nm [34]. Because of the

3 nm height difference between GRGDSP and PEG headgroups the GRGDSP headgroups on the boundary would have a larger volume to establish a lower conformational state than the GRGDSP headgroups on the interior of the GRGDSP-containing phase, where the GRGDSP headgroups are tightly packed. Therefore, a multitude of peptide conformational states could exist between the phase boundary to the interior of the GRGDSP-containing phase. This continuum of GRGDSP conformational states could eliminate integrin specificity by engaging several integrins without being selective to any one. Thus, if the 10 mol% $(C_{18})_2$GRGDSP/90 mol% PEG and the 75 mol% $(C_{18})_2$GRGDSP/25 mol% PEG films resulted in different ligand distributions or conformational differences between ligands, different integrins could be engaged.

We can therefore conclude that β_1-containing integrins mediated HUVEC adhesion to linear GRGDSP peptides better than did $\alpha_v\beta_3$ and there was a preferential engagement of $\alpha_v\beta_3$ by the looped presentation of GRGDSP compared to the linear presentation. This result is in agreement with recent studies showing that a more constrained, cyclic or looped, peptide versus a linear one exhibits a higher affinity for the $\alpha_v\beta_3$ integrin [14,15,17,38].

3.5. Effect of the synergy site PHSRN on cell adhesion and spreading

While many integrins recognize the RGD motif in the III_{10} repeat of fibronectin, the synergy site, PHSRN in the III_9 repeat, enhances $\alpha_5\beta_1$ adhesion and spreading [8]. In order to clarify the role of PHSRN, it was necessary to investigate whether PHSRN, as a secondary binding site, can support adhesion alone. Accordingly, mixed monolayers of $(C_{18})_2$PHSRN/PEG were prepared, where monolayers of $(C_{18})_2$GRGDSP/PEG served as positive controls to demonstrate that HUVEC adhere to a permissive substrate. Even as the surface concentration of PHSRN increased, cell adhesion was unaffected (Fig. 10). Cell adhesion increased as the concentration of GRGDSP ligand in the monolayer increased, while cell adhesion failed to increase as the concentration of PHSRN ligand increased. Fig. 10 demonstrates that HUVEC adhered to monolayers of PHSRN/PEG in similar fashions as to a pure PEG monolayer. Visual inspection of surfaces prepared during spreading assays showed that the few cells that did survive the washing protocol remained round on the PHSRN/PEG substrates. The non-specific interaction between the cell surface and the tethered PHSRN ligands was most likely electrostatic in nature. Results in the literature regarding the effect of PHSRN surfaces on cell adhesion vary depending on the cell type used in the experiments and the way PHSRN was presented at the interface [8,23,25,27,30,39].

Spreading assays were used to evaluate the bioactivity of multi-component peptide-functionalized LB films. Experiments were designed to determine whether tethered PHSRN peptides could modulate cell spreading on

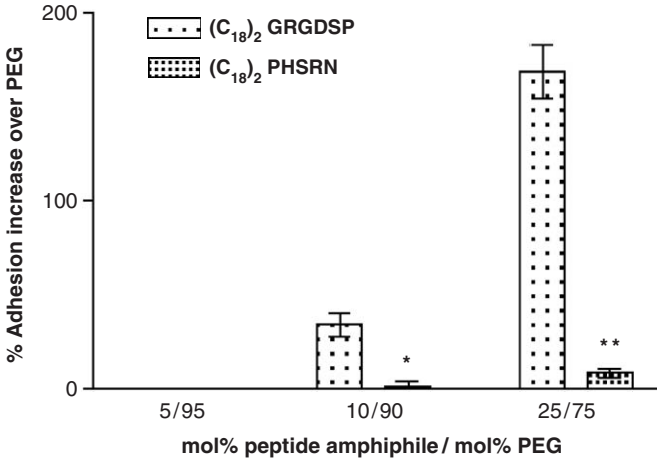

Fig. 10. Comparison of HUVEC adhesion to supported mixed monolayers of linear peptide amphiphiles and PEG, where the peptide amphiphiles were $(C_{18})_2$GRGDSP and $\alpha_5\beta_1$ synergy site $(C_{18})_2$PHSRN after 30 min incubation at 37 °C in basal medium supplemented with 0.1% BSA. Adhesion is presented as per cent increase over HUVEC adhesion to pure monolayer of PEG. $p_{10/90} < 0.001$, $p_{25/75} < 0.001$.

GRGDSP/PEG monolayers. To accomplish this, several surface concentrations of peptide amphiphiles were prepared, where the ratio of GRGDSP:PHSRN ligand at the interface was 1:1 in order to mimic the parent fibronectin molecule. In each experiment, the molar concentration of GRGDSP ligand (amphiphile in solution) remained constant in the presence and absence of PHSRN amphiphiles. Effectively, when a two-component system was converted into a three-component system, PHSRN amphiphiles replaced a percentage of the PEG molecules, while the molar concentration of GRGDSP amphiphile remained constant regardless of whether $(C_{18})_2$GRGDSP or $(C_{18})_2$GRGDSP$(C_{18})_2$ was used.

Fig. 11 demonstrates that cell areas slightly increased when an equimolar concentration of 10 mol% GRGDSP and 10 mol% PHSRN ligands was present at the interface, but that these were not significant changes. The molar concentration of GRGDSP ligand at the interface was increased to 25 mol% (Fig. 11). The data showed that cell areas increased significantly when an equimolar concentration of 25 mol% GRGDSP and 25 mol% PHSRN ligands was present at the interface. The synergy site significantly enhanced the degree of cell spreading on both presentations of the linear and looped GRGDSP ligand. The fact that the synergy site enhanced cell spreading agreed with the PHSRN discovery data. PHSRN was originally identified through hybrid adhesion/spreading assays [8]. The final set of experiments increased the surface concentration of GRGDSP ligand to 50 mol%. Because the molar ratio of GRGDSP:PHSRN must be 1:1 to mimic fibronectin, a monolayer composed of 50 mol% GRGDSP was reduced to a two-component system where the remaining 50 mol% of the surface was either PEG or PHSRN (Fig. 11). Cell area was larger on monolayers of 50 mol% $(C_{18})_2$GRGDSP/50 mol% PEG than on films of

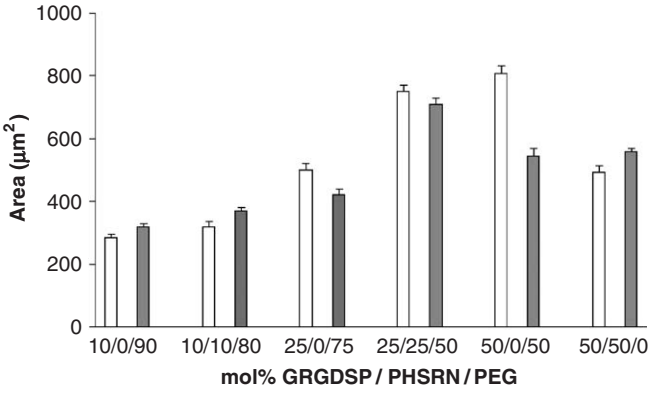

Fig. 11. HUVEC spreading on mixtures of GRGDSP. Area of spread HUVEC on supported mixed monolayers of linear or looped GRGDSP/PHSRN/PEG, with linear $(C_{18})_2$GRGDSP (white bars) and looped $(C_{18})_2$GRGDSP$(C_{18})_2$ (grey bars), after 30 min incubation at 37 °C in basal medium supplemented with 0.1% BSA (error bars represent S.E.M.).

50 mol% $(C_{18})_2$GRGDSP/50 mol% $(C_{18})_2$PHSRN, while cell area was approximately equal on films of 50 mol% $(C_{18})_2$GRGDSP$(C_{18})_2$/50 mol% PEG and 50 mol% $(C_{18})_2$GRGDSP$(C_{18})_2$/50 mol% $(C_{18})_2$PHSRN (Fig. 11). The differences between linear and looped surfaces with respect to one another and to the presence or absence of PHSRN were surprising but interesting, lending themselves to several considerations.

A potential reason that PHSRN did not enhance cell area at the 50 mol% GRDGSP ligand may have been that an excessive number of ligands were on the surface. In fibronectin RGD and PHSRN are separated by a distance of 30–40 Å [13]. In a two-component monolayer of 50 mol% $(C_{18})_2$GRGDSP/50 mol% $(C_{18})_2$PHSRN, the nearest neighbor RGDS and PHSRN ligands would be separated by the area of a single dialkyl tail. Ideal mixing and an area per dialkyl tail calculated from the LB isotherms would yield a separation distance of approximately 7 Å, if a simple circle was assumed. Similarly, in a two-component monolayer of 50 mol% $(C_{18})_2$GRGDSP $(C_{18})_2$/50 mol% $(C_{18})_2$PHSRN, the nearest neighbor RGDS and PHSRN ligands would be separated by the area of one and a half dialkyl tails, as measured from the center of the loop to the N-terminal of PHSRN. This would correspond to a separation distance of ~11 Å. In both cases, the interaction of neighboring ligands would have been too close to create a binding pocket capable of engaging $\alpha_5\beta_1$. If interactions beyond nearest neighbors were included, then there would be pairs of GRGDSP and PHSRN amphiphiles at the interface separated by the optimal distance of 30–40 Å; yet, the intervening peptide ligands would be equally as adhesive as the two ligands separated by 30–40 Å. The excessive number of ligands at less than optimal separation distances may have increased the disassociation constant of the GRGDSP/PHSRN—$\alpha_5\beta_1$ bond. If so, insufficient tension between the integrin and the substrates could have caused a decrease in cell area, which was observed for the 50 mol% $(C_{18})_2$GRGDSP/50 mol% $(C_{18})_2$PHSRN film. Cell area on 50 mol% $(C_{18})_2$GRGDSP$(C_{18})_2$/50 mol% $(C_{18})_2$PHSRN may not have changed because the crystallinity of that monolayer provided sufficient tension for cell spreading.

From the above calculations, the desired 30–40 Å spacing between ligands would result if solutions of 20 mol% $(C_{18})_2$GRGDSP/20 mol% $(C_{18})_2$PHSRN/60 mol% PEG and 25 mol% $(C_{18})_2$GRGDSP$(C_{18})_2$/25 mol% $(C_{18})_2$PHSRN/50 mol% PEG were prepared. The optimal mixture of the looped amphiphiles (25 mol% $(C_{18})_2$GRGDSP$(C_{18})_2$/25 mol% $(C_{18})_2$PHSRN/50 mol% PEG) was prepared (Fig. 11). A mixture very close to the "theoretical" mixture of linear amphiphiles (25 mol% $(C_{18})_2$GRGDSP/25 mol% $(C_{18})_2$PHSRN/50 mol% PEG) was also prepared (Fig. 11). Because the actual surface concentrations approximated the theoretical values, one could hypothesize that the optimal spacing between GRGDSP and PHSRN ligands significantly increased cell spreading. This hypothesis would explain why contributions of PHSRN were maximal at an intermediate surface concentration (25 mol% GRGDSP/25 mol% PHSRN/50 mol% PEG). The surface concentration of amphiphiles and subsequent spatial organization of the ligands may have generated the biphasic behavior.

4. Conclusions

The results shown here demonstrated that Langmuir–Blodgett films composed of GRGDSP peptide amphiphiles are model bioadhesive systems. The advantages of peptide-functionalized LB films included control of ligand density, orientation, and presentation in addition to the preparation of multi-component systems. The contribution of each variable towards creating, measuring, and defining the bioactivity of permissive substrates was assessed using adhesion, spreading, and inhibition assays. This study demonstrated that RGD presentation modulated integrin engagement and that multi-component systems could mimic an in vivo fibronectin microenvironment.

Two-component mixtures of GRGDSP/PEG amphiphiles were deposited onto solid substrates to assess the contributions of ligand presentation and density toward rendering a surface bioactive. Ligand presentation was explored using synthetic peptide amphiphiles of differing architectures. When inserted into a monolayer, $(C_{16})_2$GRGDSP presented a linear and flexible peptide while $(C_{16})_2$GRGDSP$(C_{16})_2$ presented a looped peptide structure. Adhesion of HUVEC to monolayers of $(C_{16})_2$GRGDSP/PEG and $(C_{16})_2$GRGDSP$(C_{16})_2$/PEG increased in dose-dependent manners. As the surface concentration of GRGDSP ligand increased, a higher number of cells adhered. Correspondingly, the area of spread cells increased as the surface concentration of GRGDP increased. Both presentations of GRGDSP-tethered peptides supported HUVEC adhesion and spreading. Inhibition assays revealed that different integrins discriminated between the two presentations. While

$(C_{18})_2$GRGDSP engaged β_1 integrins to a greater degree than $\alpha_v\beta_3$ integrins, $(C_{18})_2$GRGDSP$(C_{18})_2$ preferentially engaged $\alpha_v\beta_3$. Thus the architecture of tethered GRGDSP peptides is another variable that must be explored in the development of new biomaterials.

Multi-component systems were also prepared. Peptide amphiphiles based on the $\alpha_5\beta_1$ synergy site of fibronectin (PHSRN from the III_9 repeat) were incorporated into GRGDSP/PEG monolayers, such that GRGDSP:PHSRN ratio mimicked the peptide ratio in fibronectin, 1:1. The families of three-component LB films were $(C_{18})_2$ GRGDSP/PHSRN/PEG and $(C_{18})_2$GRGDSP$(C_{18})_2$/ PHSRN/PEG. The presence of the synergy site significantly enhanced cell spreading. The synergy site affected the degree of cell spreading more than the presentation of the GRGDSP ligand did.

Collectively these data demonstrated that LB films were model systems to study the contribution of non-contiguous domains to cell signaling, that multiple-tethered peptide ligands mimicked the microenvironment of the cell, and that criteria which define a surface as ''bioactive'' must be developed. The data offer numerous opportunities to develop more complex biomaterials and criteria to assess their bioactivity.

Acknowledgements

This work was partially supported by the MRSEC Program of the National Science Foundation under Award no. DMR00-80034 at the University of California, Santa Barbara and partially by the University of Minnesota MRSEC Artificial Tissues Program (DMR99-09364).

References

[1] Langer R, Vacanti JP. Tissue engineering. Science 1993;260:920–6.
[2] Healy KE, Rezania A, Stile RA. Designing biomaterials to direct biological responses. Ann NY Acad Sci 1999;875:24–35.
[3] Tirrell M, Kokkoli E, Biesalski M. The role of surface science in bioengineered materials. Surf Sci 2002;500:61–83.
[4] Dillow AK, Tirrell M. Targeted cellular adhesion at biomaterial interfaces. Curr Opin Solid State Mater Sci 1998;3:252–9.
[5] Ruoslahti E. RGD and other recognition sequences for integrins. Annu Rev Cell Dev Biol 1996;12:697–715.
[6] Hersel U, Dahmen C, Kessler H. RGD modified polymers: biomaterials for stimulated cell adhesion and beyond. Biomaterials 2003;24:4385–415.
[7] Massia SP, Hubbell JA. Vascular endothelial cell adhesion and spreading promoted by the peptide REDV of the IIICS region of plasma fibronectin is mediated by integrin $\alpha_4\beta_1$. J Biol Chem 1992; 267:14019–26.
[8] Aota S, Nomizu M, Yamada KM. The short amino acid sequence Pro–His–Ser–Arg–Asn in human fibronectin enhances cell-adhesive function. J Biol Chem 1994;269:24756–61.
[9] Altroff H, van der Walle CF, Asselin J, Fairless R, Cambell ID, Mardon HJ. The eighth FIII domain of human fibronectin promotes integrin $\alpha_5\beta_1$ binding via stabilization of the ninth FIII domain. J Biol Chem 2001;276:38885–92.
[10] Wong JY, Weng ZP, Moll S, Kim S, Brown CT. Identification and validation of a novel cell-recognition site (KNEED) on the 8th type III domain of fibronectin. Biomaterials 2002;23:3865–70.
[11] Yamada Y, Kleinman HK. Functional domains of cell adhesion molecules. Curr Opin Cell Biol 1992;4:819–23.
[12] Rezania A, Healy KE. Biomimetic peptide surfaces that regulate adhesion, spreading, cytoskeletal organization, and mineralization of the matrix deposited by osteoblast-like cells. Biotechnol Progr 1999;15:19–32.
[13] Leahy DJ, Aukhil I, Erickson HP. 2.0 Å crystal structure of a four-domain segment of human fibronectin encompassing the RGD loop and synergy region. Cell 1996;8:155–64.
[14] Pfaff M, Tangemann K, Muller B, Gurrath M, Muller G, Kessler H, et al. Selective recognition of cyclic RGD peptides of NMR defined conformation by $\alpha_{IIb}\beta_3$, $\alpha_v\beta_3$, and $\alpha_5\beta_1$ integrins. J Biol Chem 1994;32:20233–8.
[15] Xiao Y, Truskey GA. Effect of receptor–ligand affinity on the strength of endothelial cell adhesion. Biophys J 1996;71:2869–84.
[16] Pakalns T, Haverstick KL, Fields GB, McCarthy JB, Mooradian DL, Tirrell M. Cellular recognition of synthetic peptide amphiphiles in self-assembled monolayer films. Biomaterials 1999;20:2265–79.
[17] Verrier S, Pallu S, Bareille R, Jonczyk A, Meyer J, Dard M, et al. Function of linear and cyclic RGD-containing peptides in osteoprogenitor cells adhesion process. Biomaterials 2002;23:585–96.
[18] Pierschbacher MD, Ruoslahti E. The cell attachment activity of fibronectin can be duplicated by small fragments of the molecule. Nature 1984;309:30–3.
[19] Bogdanowich-Knipp SJ, Chakrabarti S, Williams TD, Dillmall RK, Siahaan TJ. Solution stability of linear vs. cyclic RGD peptides. J Pept Res 1999;53:530–41.
[20] Hruby VJ. Conformational restrictions of biologically active peptides via amino acid side chains. Life Sci 1982;31:189–99.
[21] Kao WJ, Lee D, Schense JC, Hubbell TA. Fibronectin modulates macrophage adhesion and FBGC formation: the pole of RGD, PHSRN, and PRRARV domains. J Biomed Mater Res 2001;55: 79–88.
[22] Dillow AK, Ochsenhirt SE, McCarthy JB, Fields GB, Tirrell M. Adhesion of $\alpha_5\beta_1$ receptors to biomimetic substrates constructed from peptide amphiphiles. Biomaterials 2001;22:1493–505.
[23] Hojo K, Susuki Y, Maeda R, Okazaki I, Nomizu M, Kamada H, et al. Amino acids and peptides. Part 39: A bivalent poly(ethylene glycol) hybrid containing an active site (RGD) and its synergistic site (PHSRN) of fibronectin. Bioorg Med Chem Lett 2001;11: 1429–32.
[24] Kao WYJ, Lee D. In vivo modulation of host response and macrophage behavior by polymer networks grafted with fibronectin-derived biomimetic oligopeptides: the role of RGD and PHSRN domains. Biomaterials 2001;22:2901–9.
[25] Maynard HD, Okada SY, Grubbs RH. Inhibition of cell adhesion to fibronectin by oligopeptide-substituted polynorbornenes. J Am Chem Soc 2001;123:1275–9.
[26] Susuki Y, Hojo K, Okazaki I, Kamata H, Sasaki M, Maeda M, et al. Preparation and biological activities of a bivalent poly(ethylene glycol) hybrid containing an active site and its synergistic site of fibronectin. Chem Pharm Bull 2002;50:1229–32.
[27] Aucoin L, Griffith CM, Pleizier G, Deslandes Y, Sheardown H. Interactions of corneal epithelial cells and surfaces modified with cell adhesion peptide combinations. J Biomater Sci Polym Ed 2002;13: 447–62.
[28] Mardilovich A, Kokkoli E. Biomimetic peptide-amphiphiles for functional biomaterials: the role of GRGDSP and PHSRN. Biomacromolecules 2004;5:950–7.
[29] Kokkoli E, Ochsenhirt SE, Tirrell M. Collective and single-molecule interactions of $\alpha_5\beta_1$ integrins. Langmuir 2004;20:2397–404.
[30] Feng YZ, Mrksich M. The synergy peptide PHSRN and the adhesion peptide RGD mediate cell adhesion through a common mechanism. Biochemistry 2004;43:15811–21.
[31] Benoit DSW, Anseth KS. The effect on osteoblast function of colocalized RGD and PHSRN epitopes on PEG surfaces. Biomaterials 2005;26:5209–20.

[32] Berndt P, Fields GB, Tirrell M. Synthetic lipidation of peptides and amino-acids—monolayer structure and properties. J Am Chem Soc 1995;117:9515–22.
[33] Hern DL, Hubbell JA. Incorporation of adhesion peptides into nonadhesive hydrogels useful for tissue resurfacing. J Biomed Mater Res 1998;39:266–76.
[34] Dori Y, Bianco-Peled H, Satija SK, Fields GB, McCarthy JB, Tirrell M. Ligand accessibility as means to control cell response to bioactive bilayer membranes. J Biomed Mater Res 2000;50:75–81.
[35] Hansma HG, Clegg DO, Kokkoli E, Oroudjev E, Tirrell M. Analysis of matrix dynamics by atomic force microscopy. Method Cell Biol 2002;69:163–93.
[36] Idiris A, Alam MT, Ikai A. Spring mechanics of α-helical polypeptide. Protein Eng 2000;13:763–70.
[37] Mardilovich A, Kokkoli E. Patterned biomimetic membranes: effect of concentration and pH. Langmuir 2005;21:7468–75.
[38] Dechantsreiter MA, Planker E, Matha B, Lohof E, Holzemann G, Jonczyk A, et al. N-Methylated cyclic RGD peptides as highly active and selective alpha(v)beta(3) integrin antagonists. J Med Chem 1999;42:3033–40.
[39] Fittkau MH, Zilla P, Bezuidenhout D, Lutolf MP, Human P, Hubbell JA, et al. The selective modulation of endothelial cell mobility on RGD peptide containing surfaces by YIGSR peptides. Biomaterials 2005;26:167–74.